Mechanistic Modeling of Alkaline/Surfactant/Polymer Flooding for Snorre Field from Core-scale to Larger Scale of One-Spot Pilot

Rasoul Khaledialidusti[#1], Jon Kleppe[#2], Medad Tweheyo[#3], Kjetil Skrettingland[#4]
[1, 2] *Department of Geoscience and Petroleum, NTNU, Trondheim, Norway*
[3,4] *Statoil ASA, Box 8500, 4035 Stavanger, Norway*

Abstract— *A considerable amount of oil resides in the Snorre reservoir in the North Sea. The impact of low-salinity-water flooding was investigated from core-scale using coreflood tests to larger scale of one-spot pilot using Single-Well-Chemical-Tracer (SWCT) tests before. Since the results showed a negligible amount of oil recovery, the alkaline/surfactant/polymer (ASP) flooding has been selected after the evaluation of the feasibility of all possible chemical enhanced oil recovery (EOR) methods based on the reservoir conditions. The potential of ASP has been evaluated through mechanistic modeling from core scale to large scale of one-spot pilot using SWCT test.*
First, the mechanistic modeling of ASP coreflood has been performed to make sure about the proper propagation of alkali, in-situ surfactant (soap), and surfactant. Second, the ASP injection has been also evaluated at larger scale of one-spot pilot using SWCT method. Mechanistic modeling of ASP flooding is highly sophisticated because of the complicated ASP phase behavior and the reactions that affect the process. Almost all effective reactions have been taken into account. Although low-salinity-water flooding as a standalone method could not improve oil recovery, the effect of low-salinity-water on the ASP efficiency has been studied to design and optimize the ASP method.

Keywords— *ASP flooding, Single-Well-Chemical-Tracer (SWCT) method, low-salinity-water flooding, oil saturation.*

I. INTRODUCTION

Considerable amounts of oil remain in many reservoirs such as Snorre field in the North Sea. Therefore, there is need to improve recovery of the remaining oil. The selection of which EOR method to use and the measurement of residual oil saturation (S_{or}) after is key to evaluating the success of these EOR methods. There are a number of laboratory and field methods to determine S_{or}.[1,2,3,4,5,6] The laboratory methods may not precisely predict S_{or} at the reservoir scale even when performed with extreme accuracy because core plugs may not entirely represent the gamut of properties. Therefore, field methods to determine S_{or} are more reliable. Recently, employing a combination of the field methods is proposed to determine a more accurate S_{or} measurement.[7]

In the case of Snorre field, both coreflooding experiments and field methods such as well logging and Single Well Chemical Tracer (SWCT) were conducted. The Cased hole saturation logs measurements represent the formation close to or at the well bore while SWCT technology (details are given in Appendix A) offers a method to determine S_{or} at more remote distances up to 3-15 meters from the well.[8]

From the SWCT tests, it was concluded that the potential of low-salinity-water flooding at the Snorre field is negligible, which was also verified by coreflooding results. The potential of low-salinity is often attributed to wettability alteration from oil-wet to water-wet conditions.[9,10,11] In the case of the Snorre field (Statfjord and Lunde formations); the wetting conditions are mainly neutral- to weakly water-wet, which is optimal for efficient seawater flooding.[12,13] It is with this background that chemical EOR methods have been suggested as possible alternatives for the Snorre field. In this paper, the potential of ASP as an EOR method in the Snorre field is investigated through mechanistic modeling from core scale to large scale of one-spot pilot using SWCT test.

Chemical flooding has been considered as one of the promising EOR methods, especially in the last three decades. Each of the chemicals (i.e., alkaline, surfactant, and polymer) has a specific effect on improving oil recovery. Depending on the reservoir conditions, one or a combination of these chemicals could be even more efficient. The efficiency of all chemical EOR injections especially surfactant-based methods are sensitive to parameters such as chemical slug size and concentrations, adsorption, brine salinity, temperature, and timing. The mechanisms of different chemical EOR is explained in the following.

Some steps (**Fig. 1**) should be done before performing each EOR method in full-field.[14] However, the need for a full-field implementation is not reflected. Of course we could consider field

implementation based on the results from SWCT test, but the chance of deciding full-field implementation based on SWCT test, even if 5-10 different SWCT tests have been done, is very low. Chemical flooding has high cost and risk, and a large scale field pilot will be required before a decision of full-field implementation.

Fig. 1—Sequence of EOR method evaluation.

1- Many laboratory evaluations should be performed such as phase behavior as a function of surfactant, reservoir oil, and alkali concentrations (i.e., bottle tests). Formation brine and crude oil analysis are the other parameters that have a considerable effect on the process. The properties of the candidate chemicals such as polymer with respects to the reservoir conditions should be also measured.

Due to the lack of the laboratory phase behavior data of surfactant/alkali/crude oil for the Snorre field, the measured data of a very similar crude oil and formation brine at similar temperature is used.[15] Polymer viscosity is modelled as a function of the shear rate, salinity, and a polymer concentration at the reservoir temperature.

2- From the bottle tests, many laboratory corefloods with reservoir properties should be conducted to evaluate alkali and surfactant consumption, mobility control, and oil recovery for the most attractive candidate surfactant formulations with different concentrations of chemicals.

Since this step is not also executed for the Snorre field, the available data for the Berea sandstone is used.[16]

3- Simulation of the corefloods (i.e., one of the objectives of this paper) should be done in order to designing and optimization of the process to ensure the proper propagation of high pH, effective soap, and surfactant concentrations to promote low IFT and favorable salinity gradient.

By the mechanistic modeling of the ASP flooding based on the formation rock and brine compositions, the ASP injections is designed to minimize the amount of chemicals required and costs. First, the 1D ASP coreflood, is modelled to validate the procedure of the mechanistic modeling of ASP flooding which was done by Zhao et al.[15]. Second, the feasibility of the ASP method based on the Snorre field properties including rock compositions, brine salinity, and acidic component in the crude oil is examined by the investigation of the propagation front of the chemicals using a series of 1D coreflood simulations because the simultaneous propagation of the in-situ and injected synthetic surfactant is very crucial in the success of ASP flooding. Different cases are designed to identify the key parameters and an optimum design is determined based on the simulation results.

4- SWCT tests combined with EOR technology constitute a useful monitoring technique to predict S_{or} at larger scale of one-spot pilot.

In this paper, the optimum ASP design from the coreflood simulations is also evaluated using SWCT technology. First, SWCT test #1 after waterflooding is interpreted numerically to obtain more precise S_{or} and more detailed data from the reservoir. Second, SWCT test after the ASP injection is modeled to determine S_{or} in order to evaluate the ASP injection at larger scale one-spot pilot; however, a large scale field pilot is needed to consider full-field implementation.

5- Field pilot implementation should be developed to evaluate the optimum ASP injection at larger scale than one-spot pilot. As it is mentioned, the results of the filed pilot implementation are required to decide about the full-field implementation.

The flow chart of the objectives of the paper is illustrated in **Fig. 2**.

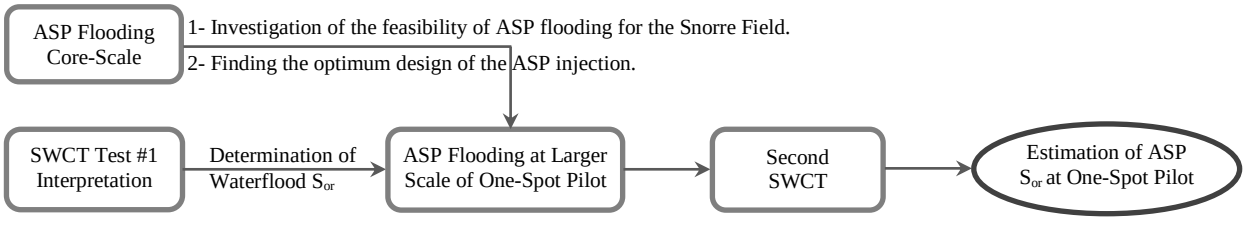

Fig. 2—Flow chart of the evaluation of ASP injection from core-scale to larger scale of one-spot pilot.

II. Chemical EOR Mechanisms

The mechanisms by which the different chemical EOR methods mobilize oil vary. Surfactants reduce the interfacial tension (IFT) between the brine and oil phases, leading to increase in the capillary number. Also, surfactants have the effect of changing the rock wettability and mobilizing oil trapped by capillary forces.

An optimum salinity of the surfactant slug is a crucial design parameter to achieve ultra-low IFT. This favorable condition happens in the salinity region of Winsor Type III microemulsion.[17,18] Due to better transport of low-viscosity microemulsion thorough porous media, it causes low-pressure gradient and reduces surfactant retention.[19] At salinity greater than the optimum salinity, a Winsor Type II microemulsion is formed, which may result in trapping the microemulsion with the residual oil. At salinity less than the optimal salinity, a Winsor Type I microemulsion is formed which has higher IFT for efficient oil mobilization.

Polymer flooding enhances oil recovery by improving the sweep efficiency and controlling the mobility. However, the performance of polymer flooding drops at harsh reservoir conditions due to high salinity and temperature. High salinity and temperature increase polymer adsorption and decrease polymer viscosity.[20,21]

Alkaline agents such as Na_2CO_3, NaOH, KOH, and $NaBO_2$ enhance oil recovery by different mechanisms. First, by lowering the IFT via the reaction with the acidic components in the crude oil that leads to the generation of soap (in-situ surfactant). Next, by changing the rock wettability toward more water-wet conditions. Last but not least, by decreasing the adsorption of anionic surfactant via increasing of pH in the active region where the surfactant has more concentration.[22]

As mentioned above, the main limitation of chemical EOR injections is harsh reservoir conditions.[21,23,24,25] For surfactants, some approaches have been suggested on how ultra-low IFT can be achieved in hard formation brines. These strategies include performing a soft water pre-flush,[26] performing salinity gradient,[27,28] developing new surfactant formulation,[29] and adding alcohol or co-surfactant.[30] Another limitation associated with chemical EOR is the high cost of chemicals.

Successful implementation of Surfactant/Polymer (SP) and Alkaline/Polymer (AP) injections is challenging and risky in reservoirs with harsh conditions and non-acidic crude oil, such as the case of Snorre field. A method based on a combination of Alkaline/Surfactant/Polymer (ASP) has also been noted to possess significant EOR benefits, and has been proved at harsh reservoir conditions.[31,32] For the Snorre field, ASP is considered as the most promising chemical EOR method. Like all chemical EOR methods, ASP flooding has uncertainties especially at harsh conditions; However, the inclusion of an alkali agent makes this method more desirable even at such conditions due to: a) reduction of surfactant and polymer adsorption on the rock surface means that less amounts of these chemicals are injected,[22] b) wettability alteration,[33,34] c) acceleration of the equilibrium time,35 and d) improving polymer hydration.[36]

Even if the amount of soap generated is negligible, the increase in pH and decrease in surfactant adsorption still impacts positively on the success of the ASP injection.[24,34] Although alkaline has a great influence on the ASP flooding, the success of this method depends on the simultaneous propagation of the alkali with surfactant and polymer.[36] Apparently, the simultaneous propagation is what promotes low IFT and a favorable salinity gradient, decreases chemical adsorption, and improves sweep efficiency. Otherwise, other EOR methods such as SP may be more efficient but the simultaneous propagation of surfactant and polymer in the presence of an alkali gives the ASP method better probability of success because soap effect on the optimum salinity of surfactant phase behavior.[37,38]

Although low-salinity-water flooding as a standalone method could not improve oil recovery on the Snorre field,[39] low-salinity-water has an impact on surfactant phase behavior, adsorption of both surfactant and polymer, and polymer viscosity.[21,40,41] Therefore, the effect of low-salinity-water on the ASP efficiency has been studied in this work to design and optimize the ASP method for the Snorre field.

Mechanistic modeling of ASP flooding is greatly sophisticated because of the complicated ASP phase behavior and the geochemical reactions that affect the process. A simplified model is proposed to overcome the difficulty of modeling of the ASP floods in UTCHEM by Delshad et al.[42]. There are some other models and simulators for the ASP flooding which are compared by Sheng34 and all of these models have pros and cons. UTCHEM is documented as on one of the best tools for the mechanistic modeling of ASP floods by Goudarzi et al.[43]. The full UTCHEM calculation flow chart is given by Kazemi Nia Korrani et al. [44] , in which the pressure equation is solved implicitly and then the component concentrations rather than saturations are solved explicitly (IMPEC) after the initialization step. Hand's rule is used to find phase saturations at each gridblock using the overall concentrations for the volume-occupying components. The effect of the gas, i.e., both solution and free gas, is neglected in our simulation. However, the free and solution gas affect the surfactant and soap phase behavior as well as the geochemical reactions in a field application,[45] depending on the reservoir pressure. For the case of Snorre, the pressure is higher than the bubble point pressure and the assumption is that the effect of gas on the surfactant and soap phase behavior is minimal. Then, in the flowchart, the phase saturations are used to calculate the relative permeability and capillary pressures. Finally, the reservoir rock and fluid properties are updated for the new component concentrations.

In this study, the geochemical module (EQBATCH) which is developed by Bhuyan[46] is used for the initial equilibrium concentrations of

aqueous, solid, and adsorbed species. Almost all essential reactions that affect the ASP flooding in this sandstone reservoir such as cation exchange, soap generating, and precipitation/dissolution reactions are taken into account by the module. In order to find the thermodynamic reaction equilibrium data for solution and solid species, PHREEQC databases is used.[47]

III. SWCT TESTS IN SNORRE FIELD

Three SWCT tests were carried out in Well P-07 of Snorre field in order to evaluate the effectiveness of low-salinity-water flooding as a possible EOR method for the field. In each test, three tracers (1-Ethyl acetate (EtAc) as a primary and reactive tracer which produces Ethanol (EtOH) as a fourth tracer; 2-n-propanol (NPA) as a backup tracer for EtAc if the amount of remained EtAc is negligible after hydrolysis reaction, and 3- isopropanol (IPA) tracer for material balance proposes) were injected. The sequences of these tests are shown in **Fig. 3**.

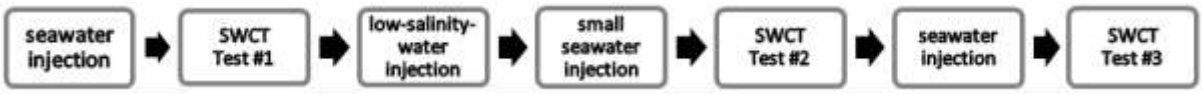

Fig. 3—Sequence of SWCT tests in Snorre field.

Before performing SWCT tests the 95 m^3 pore volumes (PV) of investigation was flooded with 11.5 PV of seawater. After this injection, the produced fluid from back production reached to around 1% measurable oil cut and then after a small flush of seawater injection SWCT test #1 was performed. After this injection, 2.3 PV of low-salinity-water was injected in order to mobilize a portion of the remaining oil after seawater-flooding. After the low-salinity-water injection and a follow up of small seawater injection, a second SWCT test, Test #2, was done to determine remaining oil saturation after flooding with low-salinity-water. Additional seawater injection of 3.8 PV was performed again and the third SWCT test, Test #3, was carried out to confirm that a possible reduction of the remaining oil saturation was not additional flooding towards S_{or}, but from change of water composition.[39] All the SWCT tests were performed with seawater in well P-07 to ensure that any changes in the tracer responses were not caused by changes in water composition. The results of these three tests are summarized in **Table 1**.

Table 1—SWCT test results in P-07 well

Test Description	Test Size (m^3)	Depth of Investigation (m)	S_{or} Measured
Test #1, Seawater S_{or}	250	9.4	0.24 ± 0.02
Test #2, Drill water S_{or}	250	9.6	0.23 ± 0.02
Test #3, Repeat S_{or}	250	9.6	0.23 ± 0.02

The apparent minor reduction in oil saturation is explained to, most likely, be caused by a minor production volume discrepancy in Test #1. Repeated SWCT test should be performed with identical displacement volumes for each measurement so that makes the quality checking of the data easiest. The production volumes should be quality checked by comparing the back-production of the inactive water tracer (e.g., NPA) which should be the same for all SWCT tests, and in case of discrepancies the production volumes has to be corrected accordingly. The injection rate/volume is known and production rate/volume is more uncertain, and it was shown that there was an error in the measured production volume in SWCT Test #1 by doing the consistency check as described by Skrettingland et al.[39] As a result, the remaining oil saturation was 0.23 from all the three SWCT tests.

IV. SNORRE FIELD DESCRIPTION

Snorre oil field is located in the North Sea 150 km from the Norwegian coastline, with original oil in place (OOIP) of 558 million Sm^3. Production from the southern and northern part of the field started via water injection as the main drive mechanism in 1992 and 2001, respectively. The main drive mechanism is currently water-alternating-gas injection that started on a large scale in 1996. Reservoir porosity and permeability varies from 0.14 to 0.32 and from 100 to 4000 md, respectively. The initial water saturation (S_w) is in the range of 0.1 □ 0.2 and the formation brine salinity is 3.43 wt%. The wettability is classified as neutral-wet to weakly water-wet in Lunde and Statfjord formations while the total clay content is in the range of 5 □ 35%. The reservoir temperature is 90°C and the initial pressure was 383 bar. The pH of the formation brine is about neutral. More details of Snorre field are mentioned by Skrettingland et al.[39] and Khaledialidusti et al.[48,49]

The formation brine, rock mineralogy, and crude oil/core properties are listed in **Tables 2**, **3**, and **4**, respectively. The rock mineral compositions were determined by X-ray-diffraction (XRD) analyses from core samples taken at a depth of 4072.0 m in well P-07.[39] To reduce on the amount of computational costs and time, only three dominant brine elements of Na^+, Cl^- and Ca^{2+} were used to represent the monovalent ions and divalent cations.

Only two principal rock solid components, i.e., quartz and kaolinite were used as input components in the simulator.

Table 2—Composition of Formation and Simulated Brine

Constituent	Formation Brine (g/l)	Positive Ion (ppm)	Negative Ion (ppm)	Total (ppm)	Simulated Brine	Total (ppm)	Simulated Element	Conc., (meq/ml)
NaCl	30.5	11998.5	18501.45	30500	NaCl	31260	Na^+	0.5348
KCl	0.23	120.6	109.37	230			Cl^-	0.5698
$NaHCO_3$	0.53	145	384.96	530			$Ca2^+$	0.0698
$CaCl_2.2H_2O$	4.17	1136.8	2010.97	3148	$CaCl_2$	3876		
$MgCl_2.6H_2O$	1.35	161.4	470.67	632				
$BaCl_2.2H_2O$	0.08	45	23.23	68				
$SrCl_2.6H_2O$	0.047	15.4	12.5	28				
Salinity (wt %)	3.43							
Ionic strength (mol/l)	0.631							

Table 3—Rock Mineral Composition (from XRD analyses)

Mineral	wt%	Clays	wt%
Quartz $[SiO_2]$	54.7	Kaolinite $[Al_2Si_2O_5(OH)_4]$	14.7
K-feldspar	16	Mica/Illite	8.8
Plagioclase	3.1	ML clay	0.7
Chlorite	1.6		
Siderite	0.3		
Pyrite	0.1		
Total	75.8	Total Clay	24.2
SUM (wt%)			100

Table 4—Oil and Core Properties

Oil Property	STO	Reservoir Oil	Core Property	
Density at 20 °C and 1 bar (g/ml)	0.829	0.825	Porosity	0.31
Viscosity at 90 °C and 6/300 bar (cp)	1.16	0.58	Brine permeability (md)	3500
Total acid number (mg KOH/g)	0.02	-	Temperature, °C	90
Total base number (mg KOH/g)	1.1	-	Residual oil saturation	0.24
IFT against seawater (mN/m)	19.1	30.1	Residual water saturation	0.1
IFT against 2000 ppm NaCl (mN/m)	19.1	29.9		

V. ASP Modeling (Reactions and Phase Behavior)

The details of the reactions and phase behavior involved in ASP modeling are included in **Appendix B**. The main parameters based on previous works by Mohammadi et al.[36], Kazemi Nia Korrani et al.[44], and Bhuyan et al.[50] are:

- ion exchange reactions with clays,
- IFT reduction as a function of soap and surfactant concentrations,
- aqueous chemical reactions,
- reaction between the acidic components of crude oil and the injected alkali to generate soap,
- effect of increasing pH on the reduction of surfactant adsorption,
- precipitation/dissolution reactions in high temperature reservoir,
- phase behavior as a function of soap and surfactant concentrations.

Accordingly, geochemical reactions and surfactant phase behavior are crucial for the ASP flooding. This section highlights the role of reservoir temperature, rock mineral components, crude oil properties, and formation brine composition on the geochemical reactions and surfactant phase behavior.

A. Reactions

The essential geochemical reactions that affect ASP flooding are taken into account. These reactions are mainly responsible for the changing of pH due to injection of alkali. Dissolution and precipitation reaction of solid minerals is modelled at high temperature conditions, as is the case for Snorre field. Na_2CO_3 is used as the alkaline agent in these simulations to reduce surfactant adsorption and to generate soap.

In-situ soap generation: The input parameter in the model for in-situ soap generation is the acid number, which determines the potential of crude oil to form soap.

Homogeneous aqueous reactions: The most important aqueous reactions in the ASP model are the buffered reactions. Here, carbonate and bicarbonate buffered solutions have been used. These reactions have a considerable effect on the amount of alkaline needed to obtain a certain pH level in an aqueous solution.

Ion exchange reactions with rock minerals: The effect of ion exchange reactions with clays has a great impact on the propagation and breakthrough time of the alkali. The main feature of these reactions is that they are reversible and relatively fast. In the ASP model, the main parameter is the cation exchange capacity (CEC) of the rock. In the case of Snorre, the exchange reaction between sodium and calcium has not modelled because the calcium concentration in the formation brine (**Table 2**) is negligible.

Dissolution and precipitation reactions: Dissolution and precipitation of solid minerals should be taken into account in high temperature reservoirs, which is the case for Snorre. Dissolution of quartz and kaolinite, the most abundant minerals in Snorre, are examples of this kind of reactions. The main source of precipitation is calcite precipitation. Dissolution of kaolinite can also lead to precipitation of analcime ($NaAlSi_2O_6H_2O$). These two precipitations reactions, plus the dissolution of quartz and kaolinite, have been modelled.

Since the aqueous solution needs enough time to equilibrate with the rock minerals during injection ignoring the solid reactions in coreflooding simulations where the fluid velocity is high enough might be valid. However, the kinetic of the minerals are significant and solid reactions should take into account at the field scale where the fluid velocity is low far from the wells. More details of the importance of the kinetic reaction are investigated by Kazemi Nia Korrani et al.[51].

B. Phase Behavior

The solubilization data at different oil concentration are modelled via Hand's rule.[52,27] The effective salinity at which the three equilibrium phases form or disappear are called lower and upper limits of effective salinity (C_{SEL} and C_{SEU}) which optimum salinity is the mean of these two limits. Optimum salinity decreases by increasing the ratio of soap to surfactant over time and this act as a favorable salinity gradient.

The key parameters for polymer and surfactant properties are also modelled via UTCHEM. These parameters for polymer include polymer solution viscosity as a function of shear rate, salinity, and polymer concentration. All transport parameters consists of permeability reduction factors as a function of permeability, polymer adsorption, cation exchange, and inaccessible pore volume are considered. The surfactant properties which are modelled in addition to microemulsion phase behavior are microemulsion viscosity, IFT, and surfactant adsorption.

The surfactant adsorption is pH-dependent between certain pH threshold values which decrease linearly with increasing pH and constant for values less than the lower threshold value and higher than the upper threshold value. The trapping number for aqueous, oil, and microemulsion (i.e., combination of both gravity and viscous forces) which was developed by Jin[53] is modeled to represent the capillary desaturation curve (CDC) and the dependency of residual saturations on IFT. The relative permeability endpoints and exponents of the relative permeability curves change as the residual saturations change at high trapping numbers (low IFT). The endpoints and exponents of the relative permeabilities are calculated using a linear interpolation between the values at low and high trapping numbers.[54] At low IFT, the relative permeability curves are assumed to be linear with no residual saturation and 1.0 for endpoints and exponents. At high IFT, the relative permeability curves are measured experimentally. Since the CDC was also unknown, these values are considered 1865, 59074, and 364, respectively based on Berea sandstone core.[16]

As it is stated, the third steps of the evaluation of the ASP flooding before performing in full-field is corefloods simulation **(Fig. 2)**. In this step, first, the 1D ASP coreflood experiments using acidic crude oil is modelled to validate the procedure of the mechanistic modeling of ASP flooding. Second, the coreflood modeling is performed based on the physical properties of the Snorre field (**Tables 2**, **3**, and **4**) to make sure about the feasibility of the ASP flooding for the Snorre field and then finding the optimum ASP design. The surfactant phase behavior and the properties of the candidate chemicals in almost the same condition with the Snorre oil field, non-acidic, are used which are given in Mohammadi.[55]

VI. ASP COREFLOOD WITH ACIDIC CRUDE OIL

The ASP coreflooding using acidic crude oil which was performed by Zhao et al.[15] is modelled with the same rock, fluid and chemical properties. The acid number of the crude oil is 0.5 mg KOH/g oil which is enough to generate in-situ surfactant. Therefore, reactions related to soap generating is taken into consideration. The coreflood configuration is vertical and the simulation model is set up exactly with the same condition. First, the ASP slug (0.3 PV) and, then, polymer drive (1.7 PV) was injected from the bottom of the core. The simulated oil recovery, oil cut, pressure drop, and effluent pH are compared with the experimental results in **Fig. 4**. As it can be seen, the simulated results show acceptable agreement with the experimental data and would be a satisfactory validation for the mechanistic modeling of the ASP flooding.

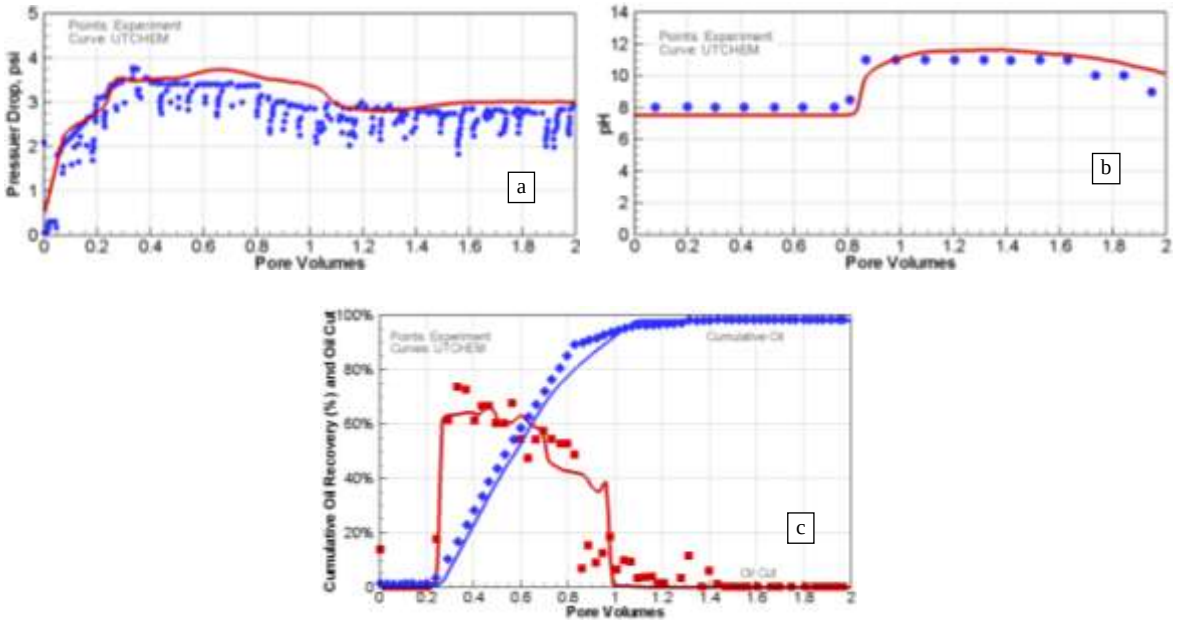

Fig. 4—Comparison of measured and simulated pressure drops (a), effluent pH (b), and oil recovery and oil cut (c).

VII. ASP COREFLOOD MODELING WITH NON-ACIDIC CRUDE OIL (SNORRE RESERVOIR PROPERTIES)

After the validation of the procedure of the ASP modeling, the same procedure is repeated with respect to the Snorre reservoir parameters. As expected, the high temperature and brine salinity conditions and the low amount of acidic component in the crude oil of the Snorre reservoir (**Table 4**) have considerable effect on the success of the ASP flooding. Dissolution of quartz and clays reactions is modelled due to the high reservoir temperature because the kinetics of the minerals has considerable impact at field scale where the fluid velocity is low far from the wells. However, these reactions can be ignored at coreflood modeling due to higher injection rate.

The reaction related to soap generation is ignored due to the negligible amount of acidic components in the Snorre crude oil. Therefore, the optimum salinity remains constant during the ASP flooding and the benefit of the favorable salinity gradient is not applicable. An ASP flood in non-acidic crude oil reservoirs is usually referred to as high-pH surfactant/polymer flood. In such reservoirs, an alkaline agent is used for other benefits such as reducing surfactant adsorption and improvement of phase behavior. Generally, high-pH surfactant/polymer flooding leads to reduction of surfactant adsorption only if the alkali propagates simultaneously with surfactant/polymer. In this section, propagation of the alkali is investigated whether ASP can be productive for the Snorre field or not.

The coreflood simulation model is set up horizontally with a length of 1 ft and diameter of 0.163 ft (**Fig. 5**). The core is initially at S_w of 0.1 with formation brine and S_{or} of 0.24 based on the results of the SWCT Test #1 (**Table 1**). The permeability, porosity, and water/oil relative permeability are considered the same as the field data (**Table 4**).

Some of the common alkali agents which used in the industry include Na_2CO_3, NaOH, and $NaBO_2$. The result of the coreflood experiments with the core from the Snorre field showed that adding NaOH (0.01 mol/L) to low-salinity-water raised the pH to approximately 12.39 Since the amount of alkali consumption increases for pH above 12, NaOH is not suitable for the Snorre field. Also, $NaBO_2$ is more favorable in carbonate reservoirs,[55] and since Na_2CO_3 is more suitable in sandstone reservoirs;[15] it was selected in this work.

Due to lack of the laboratory evaluations for the chemicals with the Snorre field conditions, phase behavior results from similar reservoir conditions are used.[15] The salinity window parameters including C_{SEL}, C_{SEopt}, and C_{SEU} for surfactant used in these simulations to match the measured oil and water solubilization ratios are 0.4, 0.535, and 0.67 (meq/ml), respectively. The surfactant adsorption level is considered to be around 0.3 mg/g rock and 0.1 mg/g rock at neutral pH and high pH of around 11, respectively.

The properties of AMPS AN-125 polymer, which have worthy compatibility with surfactants, have been used in this work.[21] The polymer solution viscosity is modelled as a function of polymer concentration, shear rate, and salinity at reservoir temperature. All parameters related to polymer transport, such as permeability reduction, polymer adsorption, and inaccessible pore volume are considered in the simulations.

The injection scheme (**Fig. 5**) was such that an ASP slug was injected at a frontal velocity of 1

ft/day for a period of time and then followed by the polymer drive-I and –II.

1- Surfactant slug including 1 wt% Na_2CO_3 and 1500 ppm AN-125 polymer

2- Polymer drive-I including 1 wt% Na_2CO_3 and 1000 ppm AN-125 polymer

3- Polymer drive-II including just 1000 ppm AN-125 polymer

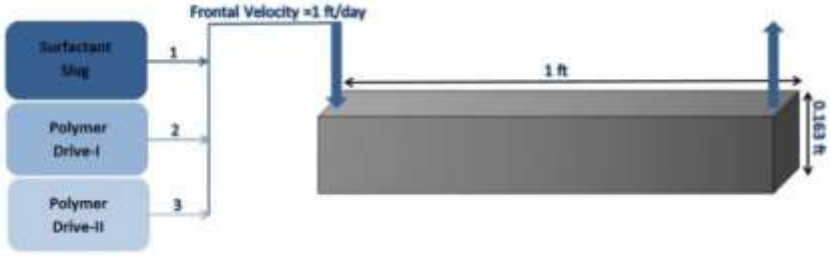

Fig. 5—Sequence of injecting the chemicals.

As stated before, the propagation of chemicals has great influence on the success of an ASP flooding. In the reservoirs including acidic crude oil, the most important condition for a successful ASP method is that both the in-situ and injected surfactant propagate simultaneously. Otherwise, the ASP method will not reach optimal conditions if the injected surfactant propagates either ahead or behind of the soap front. This is because with acidic crude oil, if the soap propagates behind the injected surfactant front, surfactant adsorption increases since the pH is not high enough. However, the adsorbed surfactant on the formation rock can partially desorb when the high-pH front reaches to the adsorbed surfactant. Conversely, if the injected surfactant moves behind of the high-pH front, the phase behavior of soap places in the Winsor Type II and can cause partial partitioning of the soap into the trapped oil. The trapped soap remains in the oil until the injected surfactant reaches the trapped soap to change its phase behavior towards optimum salinity.[36]

But, in non-acidic crude oils where there is no soap generation, the success of the ASP method can still reach optimal conditions even if the injected surfactant moves behind of the alkali front or moves simultaneously. In this condition, the propagation of the high-pH front ahead of the injected surfactant is not an issue because there is no soap to partition into the trapped oil. On the other hand, the propagation of the injected surfactant ahead of high-pH front causes exactly the same difficulty as in reservoirs with acidic crude oil components, which is to increase adsorption of the injected surfactant.

Since the Snorre crude oil is non-acidic, ASP flooding would not be optimal only when the alkali propagates behind the injected surfactant. Cation exchange reaction and CEC have strong effect on alkali consumption and propagation. Due to negligible amount of divalent cations in the formation brine (**Table 3**), only the cation exchange reaction between sodium and hydrogen is taken into account. Since the CEC of the formation rock in the Snorre oil field was not measured, the CEC from Berea sandstone is used in the simulations to examine how this parameter can affect the alkali propagation. Novosad et al.[56] stated that CEC for Berea sandstone cores vary between 0.1 and 0.4 meq/100 g rock. Therefore, two different CEC values of 0.1 and 0.3 meq/100 g rock have been studied. The effect of temperature on this reaction was neglected. **Fig. 6** shows the effect of CEC on the pH propagation at 0.25 PV. It can be seen that the higher CEC value leads to higher alkali consumption and slower propagation of the pH front, as expected.

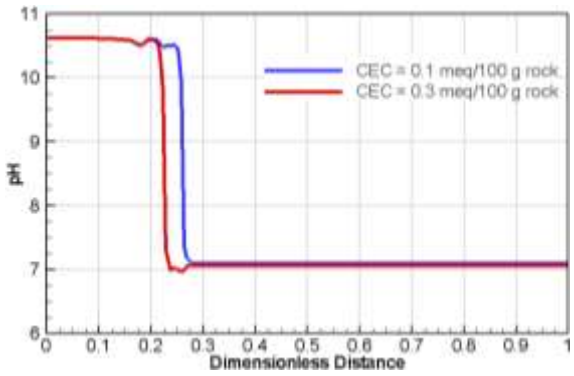

Fig. 6—pH front with different CEC values at 0.25 PV.

In a previous work, Khaledialidusti et al.[49] explored a series of 1D ASP simulations to optimize the chemical injection strategies with respect to the quantity and cost of chemicals required (**Table 5**). The following cases were explored: **a)** the propagation of high pH front and injected surfactant, **b)** the effect of concentration and slug size of the injected surfactant, **c)** the effect of injected brine salinity in all three sequences on the salinity gradient, and **d)** the effect of the second sequence, polymer drive-I.

The effect of low-salinity-water flooding on the wettability alteration is not taken into account because, as mentioned previously, the wettability in Snorre is already optimal (weakly water-wet) and low-salinity-water injection had only insignificant effect on the incremental oil recovery.[39] Low-salinity-water would also affect polymer flooding by decreasing polymer adsorption and increasing polymer viscosity.

Table 5—ASP coreflood design										
	Effect of surfactant PV %			Effect of Salinity (NaCl) in Surfactant slug		Effect of salinity in ASP coreflooding			Effect of polymer drive-I	
	5	5	10	0.342 meq/ml	0.3 meq/ml				Surfactant, 5 PV%	Surfactant, 10 PV%
Case #	**1**	**2**	**3**	**4**	**5**	**6**	**7**	**8**	**9**	**10**
Surfactant slug, PV:	0.05	0.1	0.1	0.05	0.05	0.05	0.05	0.05	0.05	0.1
Surfactant, wt%	1	0.5	1	1	1	1	1	1	1	1
Salinity (NaCl), meq/ml	0.534	0.534	0.534	0.342	0.3	0.3	0.3	0.3	0.534	0.534
1 wt% Na_2CO_3	~	~	~	~	~	~	~	~	~	~
1500 ppm AN-125	~	~	~	~	~	~	~	~	~	~
Polymer drive-I, PV:	0.2	0.15	0.15	0.2	0.2	0.2	0.2	0.2	———	———
Salinity, meq/ml=	0.534	0.534	0.534	0.534	0.534	0.3	0.3	0.25		
1 wt% Na_2CO_3	~	~	~	~	~	~	~	~		
1000 ppm AN-125	~	~	~	~	~	~	~	~		
Polymer drive-II, PV:	1.75	1.75	1.75	1.75	1.75	1.75	1.75	1.75	1.95	1.9
Salinity, meq/ml	0.534	0.534	0.534	0.534	0.534	0.534	0.3	0.2	0.534	0.534
1000 ppm AN-125	~	~	~	~	~	~	~	~	~	~
Oil recovery, % OOIP	70	55	87.8	73.2	74.8	81.5	83	84	39.6	85.9

a) *Propagation of high pH front and injected surfactant*. The propagation of high pH, injected surfactant, and oil concentration for Case #1 at 0.25 PV (after polymer drive-I) is shown in **Fig. 7a**. It can be observed that the alkaline agent has increased the pH to about 10.6, which leads to a decrease in surfactant adsorption and chemical costs. It can also be seen that both the high pH front and the injected surfactant propagates simultaneously. Hence, ASP injection can be appropriate for this sandstone reservoir. It should be mentioned that the CEC value of 0.3 meq/100 g rock has been applied, which is the worst case scenario. The cumulative oil recovery and oil cut at 0.25 PV is also shown in **Fig. 7b**. In this case, the oil recovery (%OOIP) is about 70%.

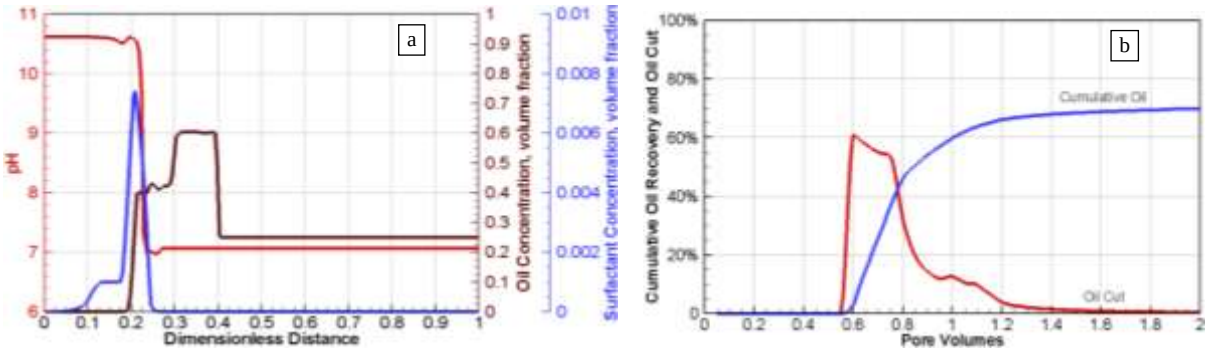

Fig. 7—Case #1: pH, injected surfactant, and oil concentration at 0.25 PV (a), and Cumulative oil recovery and oil cut (b).

b) Effect of concentration and slug size of the injected surfactant. The effect of surfactant concentration and slug size is also studied. The results (Cases #1, 2, and 3) shows that with the same PV% ((concentration, wt%)×(slug size, PV)), the large slug size has lower %OOIP than small slug size. It is because of the concept of the critical micelle concentration (CMC) that the surfactant cannot be effective for lowering IFT in the surfactant concentration lower than CMC. The results also verify that the amount of oil recovery increases by injection more slug size of chemicals in Case #3, as expected.

c) Effect of injected brine salinity. The effective salinity is another crucial parameter in order to get ultralow IFT and achieve optimum recovery by ASP flooding. A plot of salinity vs. dimensionless distance is shown in **Fig. 8** for Case #1. The figure shows that the alkaline agent has increased the effective salinity to more than C_{SEU} (Winsor Type II) where the surfactant has more concentration. This causes the surfactant to be trapped in the residual oil phase during ASP flooding. Therefore, a design of injected brine different from the formation water is required to achieve salinity gradient and ultralow IFT in the Snorre field during ASP flooding.

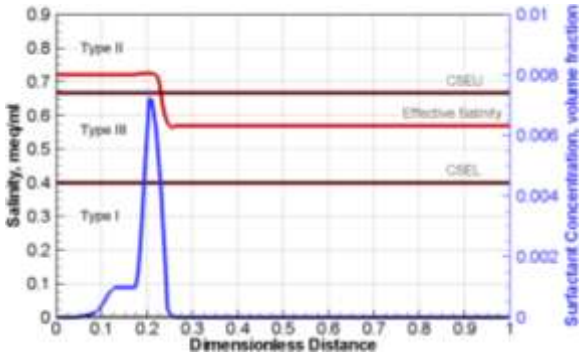

Fig. 8—Effective salinity and surfactant concentration: Case #1 at 0.25 PV.

Plots of cumulative oil recovery and oil cut vs. injected pore volumes for Cases #6 and 8 and effective salinity vs. dimensionless distance at 0.5 PV are compared in **Fig. 9**. The design of injected brine salinity in each sequence of the ASP injection for these two cases is mentioned in **Table 5**. It is illustrated that while there are two recovery periods in Case #8, the presence of this two recovery periods is hardly visible in Case #6. The first recovery period in Case #8 is started from 0.55 to 1 PV. Effective salinity profile related to this case shows that only oil bank and Winsor type III microemulsion are recovered during this period. A second recovery period in this case is started again from 1 to 1.25 PV. The second recovery period is because of the transition of the effective salinity into Winsor Type I region. As it is explained, this salinity gradient remobilizes the rest of injected surfactant in the trapped oil, decrease polymer adsorption, and increase polymer viscosity in polymer drive-II sequence. These benefits cause a second recovery period and finally additional level of oil recovery. Case #8 is specified as the optimum case in terms of oil recovery.

These observations show that while low-salinity-water injection alone could not improve oil recovery, more oil has been recovered by ASP using soft water than formation brine. Furthermore, about half of the amount of surfactant is required for ASP with soft water floods than with formation brine. This benefit makes the combination of low-salinity and ASP injections more promising for the Snorre field.

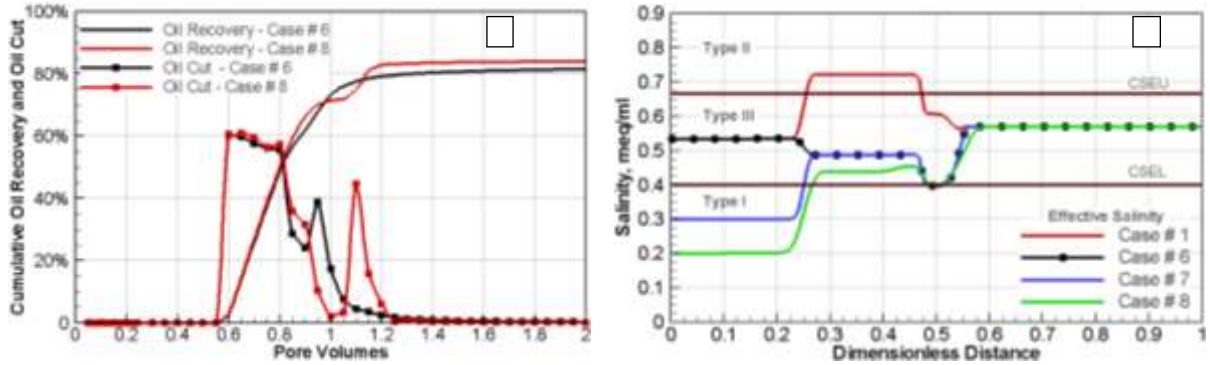

Fig. 9—Oil recovery and oil cut (a) and Effective salinity (b) at 0.5 PV.

d) Effect of the second sequence, polymer drive-I.

By comparing Cases #8, 9, and 10, it is clear that the injection of alkali behind the surfactant injection has significant impact on the success of this EOR method in Snorre. And by removing polymer drive-I in Case #9 and 10, the oil recovery was almost 45% lower in Case #9 compared to Case #8. In addition, Case #10 showed that more ASP slug volume was required to recover the same amount of oil as Case #8. This can be a result of keeping the flooding in high pH behind the active region.

VIII. INTERPRETATION OF SWCT TEST #1

The measured concentration of tracers from the SWCT Test #1 after waterflooding has been interpreted numerically to obtain a more precise S_{or} and detailed data from Snorre reservoir (P-07). As **Fig. 10** illustrates, the tracer profiles show a symmetric (Gaussian) distribution as would be expected for the thin sand region. Details of schedule, pumping sequence, pumped volumes and sampling of Test #1 were mentioned by Skrettingland et al.[39]

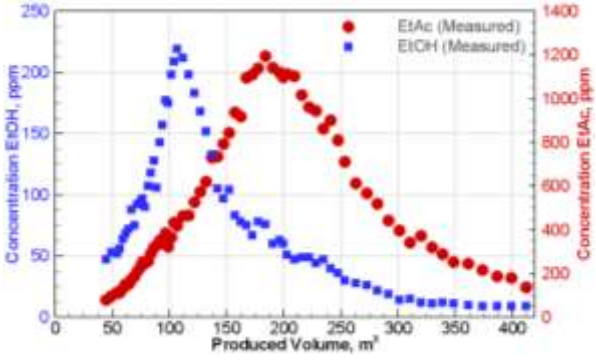

Fig. 10—Reactive (EtAc) and product (EtOH) tracer concentrations: SWCT Test #1.

In a previous work, Khaledialidusti et al.[48] presented the procedure of numerical interpretation of this SWCT test to find the best-fit parameters. There are some known and unknown parameters for the numerical interpretation of SWCT tests. The

known parameters are flow rate during the SWCT test (injection, shut-in, and production times), concentration and partitioning coefficient (K-values) of the injected tracers, well-bore radius, thickness, and porosity. The unknown parameters are radial dimension of the cells (ΔR), mechanical dispersivity, hydrolysis reaction (K_h), and S_{or}, which should be obtained in order to get the best history match. Mechanical dispersivity is considered equal to half of ΔR.[8] The numerical interpretation started with single-layer (ideal) model and then, the multi-layers (non-ideal) model was applied to obtain the better match.

1) Ideal SWCT Tests.

The ideal model started, first, with matching the modelled and measured EtAc profiles by adjusting the ΔR and K_h values. Then, the modelled EtOH profile with measured data was matched with the obtained unknown parameters by adjusting S_{or}, as shown in **Fig. 11**. The numerical interpretation indicates S_{or} of 0.24 ± 0.02 after waterflooding (Test #1).

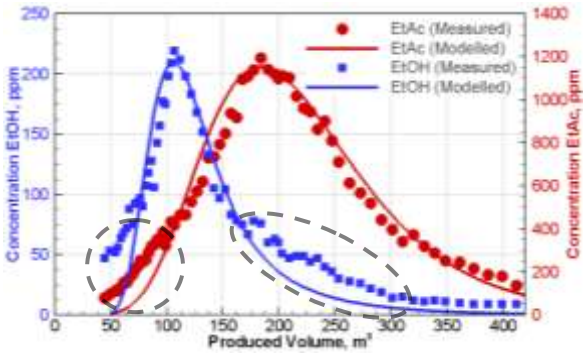

Fig. 11—Final history matches via ideal model: SWCT Test #1.

The NPA and IPA profiles were also modelled using the obtained unknown parameters and have been compared with measured profile as shown in **Fig. 12**.

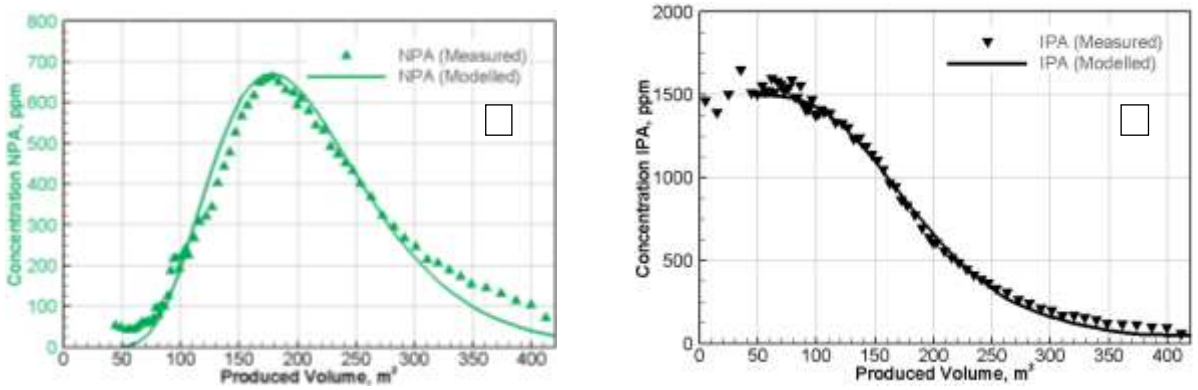

Fig. 12—NPA (a) and IPA (b) profiles using the ideal model: SWCT Test #1.

While the modelled ideal tracer profiles shows almost a perfect match, there is still some deviation between the measured and modelled profiles at the tail of the curves (**Fig. 11**), which is because of non-ideality effects. In most reported SWCT tests in different reservoirs have not reflected ideal tracer profiles.[8] The departure of a real test from ideal behavior could be explained briefly as follows:

- **Fluid drift**: different streamlines around the test well between injection and production processes arise due to pressure gradient across the field. This leads to relocation of the tracers (fluid drift) during the shut-in period while it is assumed that tracers are stationary.[8,6] To determine the amount of fluid drift in each test, the measured cover tracer (NPA) and ester (EtAc) profiles should be superimposed and the separation between these profiles determines the amount of fluid drift. As **Fig. 13** shows, there is no fluid drift in Test #1.

- **Gas lift**: due to higher vapor pressure in some SWCT tests, the EtAc could be stripped from the produced water by gas. One example of this phenomenon was observed by DeZabala et al.[57]. In tests with gas lift, the NPA profile should be used instead of the EtAc profile to interpret the test. As it is illustrated in **Fig. 13**, gas lift cannot be a source of the non-ideality behavior observed in Test #1.

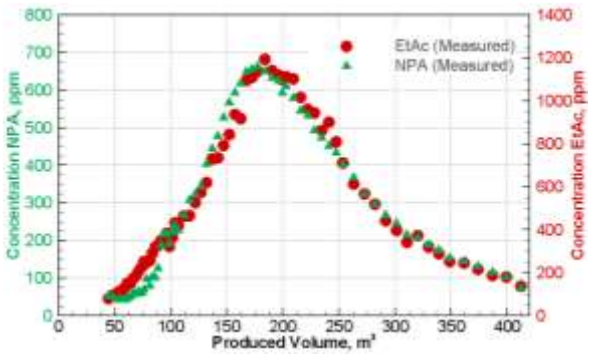

Fig. 13—Comparison of NPA and EtAc production profiles: SWCT Test #1.

- **Cross-flow**: small pressure differences within individual layers could lead to traveling of fluid with tracers between the layers during shut-in period. This could cause transportation of one tracer slug back toward the well and the other tracer slug away from the well.[8,58]

- **Flow irreversibility in layered test zones**: individual layers may accept different fractions of the injected fluid than they return to the well bore during production. Higher-pressure sub-zones produce more fluid during production than they accept during injection. Conversely, lower-pressure sub-zones produce less fluid during production than they accept during injection. This phenomenon could lead to early arrival of the tracer bank from higher-pressure layers and late arrival from lower-pressure layers.[8,58]

- **Complex pore system effects**: non-equilibrium flow conditions in carbonate and fractured sandstone reservoirs usually causes distorted tracer profile shapes.[8,59] Ester profiles arrive earlier than expected with extended tailing and can be extensive in some cases depending on lithology and distribution of the pore space.

The main challenge in interpreting non-ideal tests is to recognize the key sources of non-ideality behavior. Based on the possible reasons mentioned above and on previous research,[8,57,58,60] flow irreversibility in layered test zones has been considered as the cause for the minor non-ideal behavior observed in the Snorre SWCT Test.

2) Non-ideal SWCT Tests.

The simulation of non-ideal tests includes some new unknown parameters in addition to the unknown parameters of ideal tests. These new unknown parameters are: 1) the number of layers in the test zone, 2) the fraction of total volume of fluid injected and produced from each layer, and 3) the S_{or} for each layer.

These layering parameters are not unique to match the tracer profiles. In Test #1, three-layer model was applied to consider the non-ideality effects. Each layer was considered as a separate and non-communicating layer and the results of each layer were combined to get a single measured profile, as shown in **Fig. 14**. The procedure of the non-ideal model was such that, first, the fraction of total fluid injected and produced from each layer was changed by trial and error until the best-fit model with the ΔR and K_h from the ideal model was obtained. Finally, the S_{or} was determined by trial and error to match the modelled and measured EtOH profile which is considered constant in each layer.

The results are summarized in **Fig. 14**. As it can be seen, the main layer, early layer, and late layer accepted and produced 52%, 17%, and 31% of the total injected tracer, respectively. In order to obtain the EtOH best fit, the S_{or} equal to 0.22, 0.24, and 0.26 were used as input values in the main layer, early layer, and late layer, respectively.

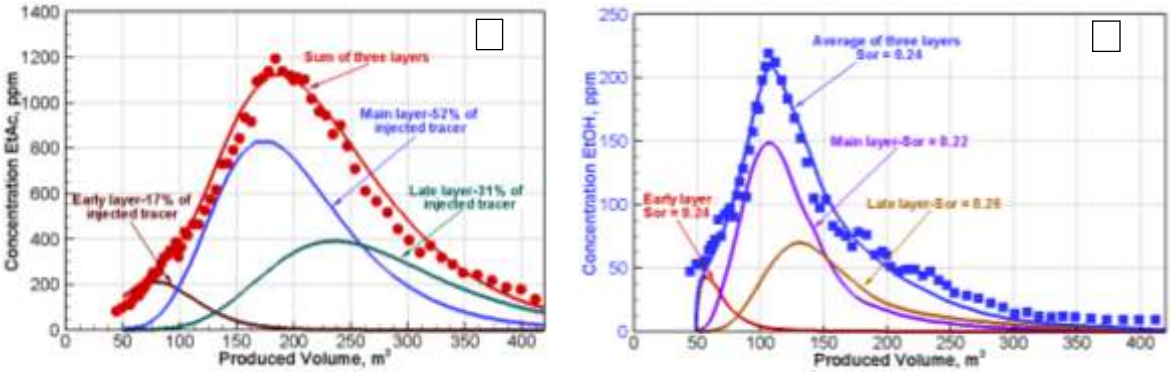

Fig. 14—EtAc (a) and EtOH (b) profiles using non-ideal model: SWCT Test #1.

IX. ASP INJECTION AT LARGE SCALE: ONE-SPOT PILOT

The effect of the ASP injection at one-spot pilot (P-07) was studied using SWCT test modeling. The volume of ASP slug is about 17% of the volume of the injected tracers and is followed by polymer drive-I and -II, exactly with the same concentration performed in the coreflood simulation (**Table 5**). The ASP slug was pushed by the chase water in four days.

The effect of the combination of low-salinity-water with the ASP flooding was also investigated based on the achieved optimum design (Case #8) in the coreflood simulations.

The capillary number is incorporated in the model by taking into account the effect of ASP on the reduction of IFT and residual oil (CDC curve). The amount of IFT reduction greatly depends on the surfactant concentration and strong desaturation occurs only in ultra-low IFT close to 10^{-3} mN/m. Since the concentration and effectiveness of the ASP slug changes due to mixing, dispersion, and surfactant adsorption phenomena, the IFT drops across the formation. In order to represent this effect, the simulated IFT distribution across the main layer of the formation during the ASP injection is illustrated in **Fig. 15**. It can be seen that the IFT across the formation changes during injection time. Therefore, complete desaturation cannot be anticipated with a short ASP slug in a region with larger radius of investigation.

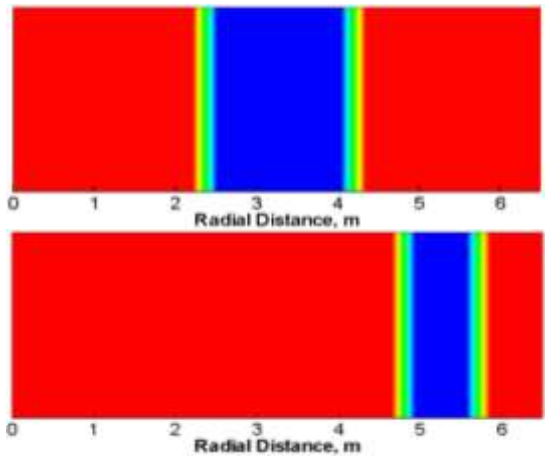

Fig. 15— IFT distribution across the main layer (blue = 10^{-3} mN/m; red = 1 mN/m).

The surfactant and polymer concentrations at the end of polymer drive-I for two different cases of ASP injection, Cases #1 and 8, are shown in **Fig. 16**. It is illustrated that while the maximum surfactant concentration (0.003 volume fraction) is significantly lower than the injected value (0.01 volume fraction), the maximum polymer concentration ((0.1 - 0.15) wt%), is closer to the injected value (0.15 wt%). The loss in surfactant concentration could be because of adsorption. It can also be seen that the surfactant concentration in the case of salinity gradient injection (Case #8) is more than the case of formation brine salinity (Case #1) at the same time. On the other hand, this difference is not very distinguishable in polymer concentration. Therefore, salinity gradient has stronger effect on the performance of the surfactant than on the polymer.

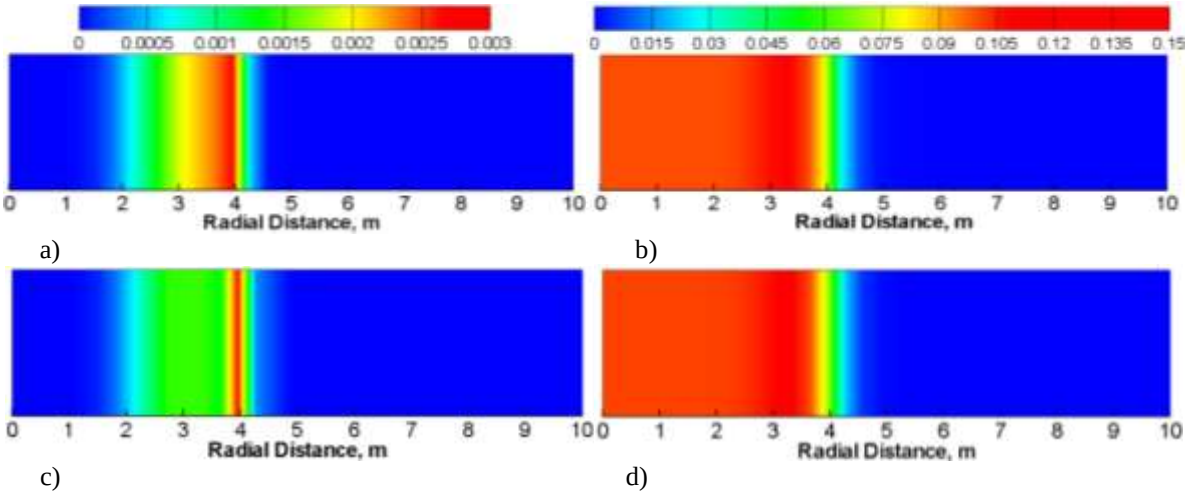

Fig. 16— Surfactant and polymer concentrations in the main layer after polymer drive-I: (a) and (b) surfactant and polymer concentrations in salinity gradient, and (c) and (d) surfactant and polymer concentrations in formation brine.

X. Second SWCT Test Modeling

The second SWCT is modelled to determine S_{or} of the ASP flooding of one-spot pilot (P-07). The test has been modelled with the same tracers, design (displacement volumes), and layer configuration as Test #1. By doing that, it is important to ensure the following: **a)** that the tracer test will not result in erroneously high residual oil saturation to ASP flooding, **b)** that the SWCT-volumes will be the same for all SWCT tests to ensure worthy quality check of the measured field data that the measured saturation change in field tests are real and not due to field volume measurement error, and **c)** that the tracers be injected to reach the end of the zone swept by the ASP flood and not where higher oil saturations exist.

To illustrate this note, **Fig. 17** shows a one-dimensional plot of the EtAc, EtOH, and surfactant concentrations for the main layer at the end of the shut-in period. As it can be seen, the EtAc reached to the investigation region where waterflood oil saturation is swept by the surfactant at the end of shut-in time. This plot clearly shows the tracer concentration terminates prior to reaching the un-swept oil, which is the objective of the SWCT test design.

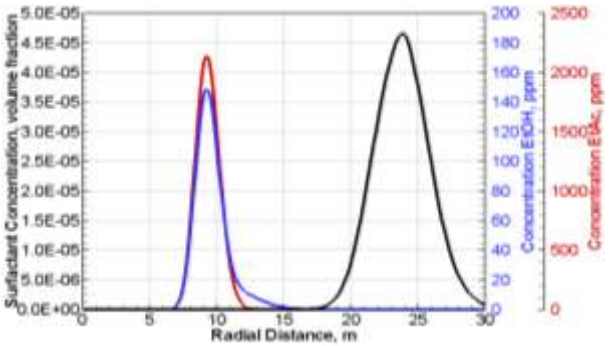

Fig. 17—Tracer and surfactant concentrations after shut-in time.

The tracer concentrations of the second test after the ASP injection for Case #8 are compared with Test #1 for all three layers in **Fig. 18**. As it can be seen and as discussed earlier, because of the reversibility nature of the unreacted ester (EtAc),

reduction in S_{or} does not affect the position of this ester peak. However, changing the S_{or} affects the position of the product tracer (EtOH) peak. The figure shows that the EtOH peak shifted to the right in the second test, which is interpreted as a result of lower S_{or}. The final result of modelled tracer concentrations of the second test is shown in **Fig. 19**.

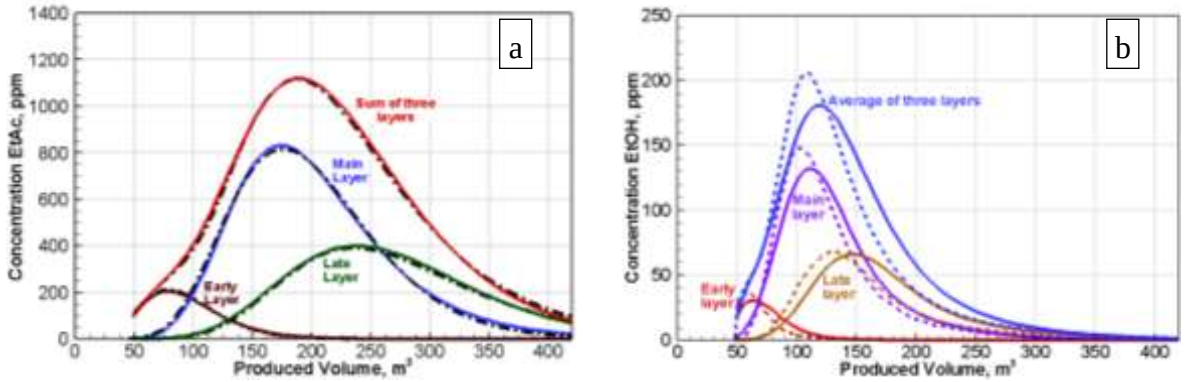

Fig. 18—Modelled EtAC (a) and EtOH (b) concentrations – Test #1 (dashed lines) and second test (solid lines).

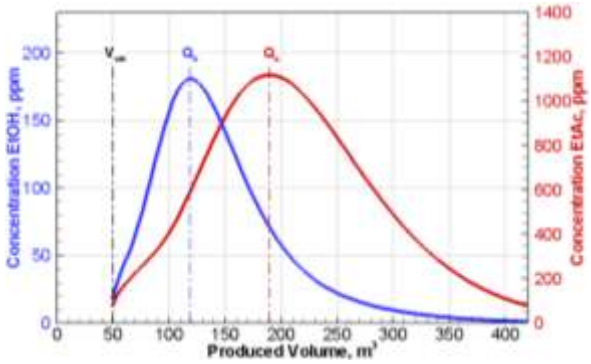

Fig. 19—EtAC and EtOH Concentration: Second SWCT test after ASP Injection with Salinity Gradient.

In order to evaluate the effect of the designed salinity gradient on the ASP injection of the one-spot pilot (P-07), the achieved tracer profiles are compared with the tracer results of the ASP injection with formation salinity brine in **Fig. 20** and **Table 6**. The results show that the EtOH in the case of formation brine salinity was produced back faster than the case of designed salinity gradient, which is because of higher S_{or} in the investigation region. The S_{or} has been calculated using **Eqs. (A-1)** and **(A-2)**. The results show that while S_{or} of the ASP flooding with formation brine is almost 0.21, the design salinity gradient decreases S_{or} to almost 0.18. Thus, it can be concluded from these simulations that while low-salinity-water injection alone could not improve oil recovery in P-07, the combination of the designed low-salinity-water with ASP injection could lead to more oil recovery.

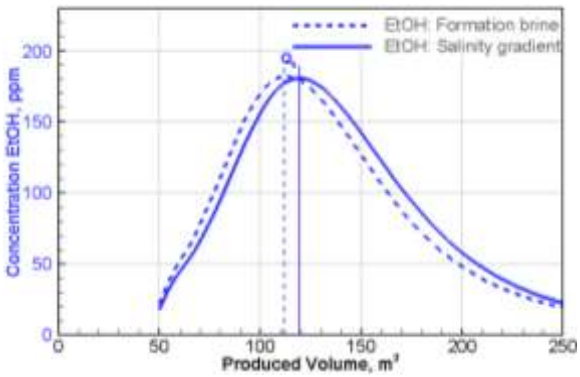

Fig. 20—EtOH Concentrations: Second SWCT test.

Table 6—ASP Residual oil saturation

	Q_a, (m^3)	Q_b, (m^3)	V_{wb}, (m^3)	β	$S_{or} = \frac{\beta}{(\beta + K)}$
Formation Brine Salinity	190	113	50	1.222	0.2099
Salinity Gradient	190	119	50	1.028	0.1828

XI. Summary and Conclusions

The potential of ASP flooding at Snorre field has been investigated through mechanistic modeling from core-scale to large scale of one-spot pilot. The SWCT method has been modelled to determine S_{or} at one-spot pilot. For mechanistic modeling, the aqueous reactions, alkali/rock interactions, and phase behavior of soap and surfactant mixtures have been taken into account. Coreflood simulations have been done to validate the ASP model to ensure propagation of chemicals, and hence the feasibility of ASP for the Snorre field. Previous work had showed insignificant impact of low-salinity-water flooding both in the laboratory and SWCT test pilot. However, the simulation results show that the ASP flooding could be a promising method to improve more oil recovery in Snorre.

Since the acidic components in Snorre crude oil are negligible, the alkali is not able to generate soap and as a result, the salinity gradient is not applicable for the ASP flooding. Therefore, the salinity gradient

has been designed for the different sequences of the ASP injections. The results show while low-salinity-water injection could not improve oil recovery in P-07, the combination of the designed low-salinity-water with the ASP injection lead to more oil recovery.

ACKNOWLEDGMENT

This project was supported by a Joint industry research project (project no. 215660/E30), financed by the Research Council of Norway, ConocoPhillips, ENI, Engie, Lundin Norway, Restrack, Saudi Aramco, Statoil and Wintershall. Financial support as well as technological input from the research project partners is gratefully acknowledged. The authors would also like to acknowledge Institute for Energy Technology (IFE) (http://www.ife.no) who hosted the project and the leadership and the resources and staff of the Department of Geoscience and Petroleum at the Norwegian University of Science and Technology.

Appendix A - Theory of SWCT Method

This method was first developed by Exxon in 1971[61] to measure saturation functions farther away from the borehole in watered out reservoirs. Many field tests have verified the reliability and applicability of this technique.[61,62] More details of the evaluation and comparison of this method with other methods to determine S_{or} are reviewed by Teklu et al.[5] and Khaledialidusti et al.[6,63, 64].

To determine S_{or} using the SWCT test, the zone must first be waterflooded to displace any mobile oil away from the wellbore, thereby placing the investigated pore space at residual oil saturation. The volume of this waterflood should be sufficient to ensure adequate Buckley-Leverett displacement of any extant mobile oil outside of the desired radius investigated by the SWCT test. Once the zone has been waterflooded and confirmed (by brief flowback) to be at residual oil saturation, a 1% solution of a hydrolyzing, partitioning ester dissolved in produced water is injected into the test well. This slug, or "ester bank," typically comprises the first 20% of the total SWCT test injection. This ester bank injection is followed by a slug of produced water (i.e., the "push bank") that comprises the remaining 80% of the SWCT test injection. The purpose of the push bank is to displace the preceding ester bank away from the wellbore and out to the maximum radial depth of investigation. The entirety of the SWCT test injection is also tagged with a conservative, non-partitioning tracer at low concentrations (e.g., 0.25%) so as to be able to calculate the material balance of the SWCT test recovery during the production stage.

After injection, the well is shut in for a period of 1 to 10 days, depending primarily on temperature and the choice of ester species. During this shut-in period, the ester hydrolyzes via reaction with the formation water to produce a non-partitioning product alcohol tracer. At the end of the shut-in period, the well is placed on production and samples of the produced water are collected at the wellhead and analyzed for tracer concentration.

During production, the non-partitioning product alcohol is able to bypass the residual oil phase and travel at the same Darcy velocity as the entraining formation water back to the wellbore. By comparison, the partitioning ester travels at a slower Darcy velocity owing to its thermodynamic tendency to partition into the residual oil phase. The result of this partitioning effect is an observable separation between the volumes at which the peaks of the product alcohol and ester tracers are produced, as illustrated in **Fig. (A-1).**

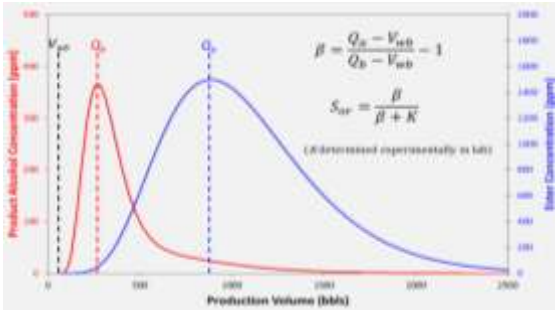

Fig. (A-1)—Hypothetical SWCT test tracer-concentration profiles to determine S_{or}.[7]

The data required for successful interpretation of an SWCT test include the tracer concentration profiles generated during the test production and the oil-water partitioning coefficient of the injected ester (K). This partitioning coefficient is typically measured in the laboratory with samples of oil and brine produced from the test well. Once the K-value is known and the tracer profiles are generated from the test production, S_{or} is measured by calculating the retardation factor β, which represents the separation between the ester and product alcohol production profiles, as shown in **Eq. (A-1)**:

$$\beta = \frac{Q_a - V_{wb}}{Q_b - V_{wb}} - 1 \qquad \text{(A-1)}$$

Where Q_a and Q_b are the volumes at which the statistical peak concentrations of the ester and product alcohol tracers are produced, respectively, and V_{wb} is the wellbore volume. Once β is determined, S_{or} is calculated according to **Eq. (A-2)**:

$$S_{or} = \frac{\beta}{\beta + K} \qquad \text{(A-2)}$$

Appendix B - Reactions and Phase Behavior

- **Reactions:** All kind of reactions that have been modelled are:

In-situ soap generation: The acid number is the amount of KOH to neutralize the acid in oil and is expressed in mg KOH/g oil. In UTCHEM, the following reactions are modelled for soap generation:[50]

a) The partitioning of acid component between crude oil and aqueous phase:

$$HA_o \overset{K_D}{\Leftrightarrow} HA_w \quad \text{(B-1)}$$

$$K_D = \frac{HA_w}{HA_o} \quad \text{(B-2)}$$

Where HA_o and HA_W are the concentration of acid in the crude oil and water, respectively. K_D is the portioning coefficient.

b) Dissociation of acid components in the aqueous phase in the presence of alkali to produce soap (i.e., soluble anionic surfactant (A^-)):

$$HA_w \overset{K_a}{\Leftrightarrow} H^+ + A^- \quad \text{(B-3)}$$

$$K_a = \frac{(H^+)(A^-)}{HA_w} \quad \text{(B-4)}$$

Here, K_a is the reaction constant. This reaction is one of the most important sources to consume the alkaline since the alkali uses OH^- to generate soap by the following reaction:

$$HA_w + OH^- \overset{K_a}{\Leftrightarrow} H_2O + A^- \quad \text{(B-5)}$$

Homogeneous aqueous reactions: Carbonate and bicarbonate buffered solutions are the most common type of aqueous reactions, as shown in **Eqs. (B-6)** thorough **(B-8)**:

$$H_2O \Leftrightarrow H^+ + OH^- \quad \text{(B-6)}$$

$$H^+ + CO_3^{2-} \Leftrightarrow HCo_3^- \quad \text{(B-7)}$$

$$2H^+ + CO_3^{2-} \Leftrightarrow H_2CO_3 \quad \text{(B-8)}$$

Ion exchange reactions with rock minerals: Exchange reactions occur between monovalent and multivalent cations. This leads to the release of multivalent cations, which have considerable effect on the phase behavior. The major ion exchanges reactions involve hydrogen/sodium and sodium/calcium. The exchange reaction between sodium and calcium is not modelled if calcium concentration in the formation brine is negligible. In this work, the dominant exchange reaction is between sodium and hydrogen on the clay surface, and is modelled as shown in **Eq. (B-9)**:

$$\overline{H}^+ + Na^+ + OH^- \Leftrightarrow \overline{Na}^+ + H_2O \quad \text{(B-9)}$$

Where $\overline{H}^+$ and $\overline{Na}^+$ are the adsorbed ions on the rock.

Dissolution and precipitation reactions:

Eq. (B-10) is the reaction for calcite precipitation:

$$Ca^{2+} + CO_3^{2-} \Leftrightarrow CaCO_3 \quad \text{(B-10)}$$

The dissolution of quartz at pH values below 9 is presented in **Eq. (B-11)**:

$$SiO_2 + 2H_2O \Leftrightarrow H_4SiO_4 \quad \text{(B-11)}$$

At higher pH values of about 12, the dissolution of quartz is presented in **Eq. (B-12)**:

$$H_4SiO_4 \Leftrightarrow H_3SiO_4^- + H^+ \quad \text{(B-12)}$$

The dissolution of kaolinite at high pH, which can result in generation of aqueous species, is presented in **Eq. (B-13)**:

$$Al_2Si_2O_5(OH)_4 + 4OH^- + 3H_2O \Leftrightarrow 2Al(OH)_4^- + 2H_3SiO_4^- \quad \text{(B-13)}$$

And, the dissolution of kaolinite can lead to the precipitation of analcime as shown in **Eq. (B-14)**:

$$Al_2Si_2O_5(OH)_4 + 2Na^+ + 2OH^- + 2H_4SiO_4 \Leftrightarrow 2NaAlSi_2O_6H_2O\ (Analcime) + 5H_2O \quad \text{(B-14)}$$

- **Phase Behavior.** To model the variation in C_{SEL} and C_{SEU} limits of the Winsor Type III region as a function of soap and injected synthetic surfactant concentration, a nonlinear mixing rule was used in UTCHEM.[46]

$$\ln S_M^* = X_{soap} \ln S_{soap}^* + X_{surfactant} \ln S_{surfactant}^* \quad \text{(B-15)}$$

where S_M^*, S_{soap}^*, and $S_{surfactant}^*$ are the optimum salinities of the mixture, soap, and surfactant, respectively. X_{soap} and $X_{surfactant}$ are soap and surfactant mole fractions.

UTCHEM batch calculation is used to obtain the soap concentration using the reactions given in **Eqs. (B-1)** thorough **(B-8)**. The calculation of phase behavior parameters such as salinity limits of Winsor Type III is performed for the entire range of the oil and alkali concentrations in order to provide these parameters for all the experimental data points. After getting the amount of generated soap from UTCHEM batch, the amount of mole fraction of the soap and the injected surfactant are calculated by having their molecular weights. The optimum oil solubilization (i.e., the oil solubilization at optimum salinity) ratio is calculated via a linear mixing rule using **Eq. (B-16)**; however, the experimental data showed that this ratio can obtain from logarithmic mixing rule.

$$\sigma_M^* = X_{soap} \cdot \sigma_{soap}^* + X_{surfactant} \cdot \sigma_{surfactant}^* \quad \text{(B-16)}$$

Where σ_M^*, σ_{soap}^*, and $\sigma_{surfactant}^*$ are optimum oil solubilization ratio of the mixture, soap, and surfactant, respectively.

REFERENCES

[1] Kidwell, C. M., & Guillory, A. J. (1980, November 1). A Recipe for Residual Oil Saturation Determination. Society of Petroleum Engineers. doi:10.2118/8451-PA.

[2] Donaldson, E. C., & Staub, H. L. (1981, January 1). Comparison of Methods for Measurement of Oil Saturation. Society of Petroleum Engineers. doi:10.2118/10298-MS.

[3] Blackwell, R. J. (1985, January 1). An Overiew of In-Situ Methods for Determining Remaining Oil Saturations. Society of Petroleum Engineers. doi:10.2118/13702-MS.

[4] Chang, M. M., Maerefat, N. L., Tomutsa, L., & Honarpour, M. M. (1988, March 1). Evaluation and Comparison of Residual Oil Saturation Determination Techniques. Society of Petroleum Engineers. doi:10.2118/14887-PA.

[5] Teklu, T. W., Brown, J. S., Kazemi, H., Graves, R. M., & AlSumaiti, A. M. (2013, March 23). A Critical Literature Review of Laboratory and Field Scale Determination of Residual Oil Saturation. Society of Petroleum Engineers. doi:10.2118/164483-MS.

[6] Khaledialidusti, R., Kleppe, J., & Enayatpour, S. (2014, December 10). Evaluation and Comparison of Available Tracer Methods for Determining Residual Oil Saturation and Developing an Innovative Single Well Tracer Technique: Dual Salinity Tracer. International Petroleum Technology Conference. doi:10.2523/17990-MS.

[7] Khaledialidusti, R., Enayatpour, S., Badham, S.J., Carlisle, C.T., Kleppe, J. (2015c, October 20). An innovative technique for determining residual and current oil saturations using a combination of Log-Inject-Log and SWCT test methods: LIL-SWCT. J. Pet. Science and Engineering, pp. 618–625. doi:10.1016/j.petrol.2015.10.023.

[8] Deans, H. A., Carlisle, C.T. (2007). The Single-Well Chemical Tracer Test - A Method for Measuring Reservoir Fluid Saturations In-Situ. In L. W. Lake (Ed.), Petroleum Engineering Handbook (Vol. V, pp. 615-649). Richardson, TX: Society of Petroleum Engineers.

[9] Morrow, N. R., Tang, G. Q., Valat, M., Xie, X. (1998). Prospects of improved oil recovery related to wettability and brine composition. J. of Pet. Sci. Eng. 1998, 20, 267–276.

[10] Lager, A., Webb, K. J., Black, C. J. J., Singleton, M., Sorbie, K. S. (2006). Low Salinity Recovery – An Experimental Investigation. SCA2006-36, International Symposium of the Society of Core Analysts, Trondheim, Norway, September 2006.

[11] Ligthelm, D. J., Gronsveld, J., Hofman, J., Brussee, N., Marcelis, F., & van der Linde, H. (2009, January 1). Novel Waterflooding Strategy By Manipulation Of Injection Brine Composition. Society of Petroleum Engineers. doi:10.2118/119835-MS.

[12] Skauge, A. and Ottesen, B. 2002. A Summary of Experimentally Derived Relative Permeability and Residual Saturation on North sea Reservoir Cores. Paper SCA 2002-12 presented at the International Symposium of the Society of Core Analysis, Monterey, California, USA, 22-25 September.

[13] Jadhunandan, P. P., & Morrow, N. R. (1995, February 1). Effect of Wettability on Waterflood Recovery for Crude-Oil/Brine/Rock Systems. Society of Petroleum Engineers. doi:10.2118/22597-PA.

[14] Stoll, W. M., al Shureqi, H., Finol, J., Al-Harthy, S. A. A., Oyemade, S. N., de Kruijf, A., … Faber, M. J. (2011, December 1). Alkaline/Surfactant/Polymer Flood: From the Laboratory to the Field. Society of Petroleum Engineers. doi:10.2118/129164-PA.

[15] Zhao, P., Jackson, A., Britton, C., Kim, D. H., Britton, L. N., Levitt, D., & Pope, G. A. (2008, January 1). Development of High-Performance Surfactants for Difficult Oils. Society of Petroleum Engineers. doi:10.2118/113432-MS.

[16] Delshad, M. (1990, December). Trapping of Micellar Fluids in Berea Sandstone. Ph.D thesis, The University of Texas at Austin, Austin, Texas, USA.

[17] Winsor, P.A. (1954). Solvent Properties of Amphiphilic Compounds. London: Butterworth's Scientific Publications.

[18] Healy, R. N., Reed, R. L., & Stenmark, D. G. (1976, June 1). Multiphase Microemulsion Systems. Society of Petroleum Engineers. doi:10.2118/5565-PA.

[19] Levitt, D., Jackson, A., Heinson, C., Britton, L. N., Malik, T., Dwarakanath, V., & Pope, G. A. (2009, April 1). Identification and Evaluation of High-Performance EOR Surfactants. Society of Petroleum Engineers. doi:10.2118/100089-PA.

[20] Moradi-Araghi, A., & Doe, P. H. (1987, May 1). Hydrolysis and Precipitation of Polyacrylamides in Hard Brines at Elevated Temperatures. Society of Petroleum Engineers. doi:10.2118/13033-PA.

[21] Levitt, D., & Pope, G. A. (2008, January 1). Selection and Screening of Polymers for Enhanced-Oil Recovery. Society of Petroleum Engineers. doi:10.2118/113845-MS.

[22] Hirasaki, G., & Zhang, D. L. (2004, June 1). Surface Chemistry of Oil Recovery From Fractured, Oil-Wet, Carbonate Formations. Society of Petroleum Engineers. doi:10.2118/88365-PA.

[23] Tabary, R., Douarche, F., Bazin, B., Lemouzy, P. M., Moreau, P., & Morvan, M. (2012, January 1). Design of a Surfactant/Polymer Process in a Hard Brine Context: A Case Study Applied to Bramberge Reservoir. Society of Petroleum Engineers. doi:10.2118/155106-MS.

[24] Tabary, R., Bazin, B., Douarche, F., Moreau, P., & Oukhemanou-Destremaut, F. (2013, March 10). Surfactant Flooding in Challenging Conditions: Towards Hard Brines and High Temperatures. Society of Petroleum Engineers. doi:10.2118/164359-MS.

[25] Delbos, A., Tabary, R., Chevallier, E., & Moreau, P. (2014, December 10). Surfactant-Polumer Flooding in Hard Brines and High Temperature Reservoirs. International Petroleum Technology Conference. doi:10.2523/18208-MS.

[26] Chiou, C.S. and Chang, H.L. (1978, February 26). Preflood Design for Chemical Flooding - A Study on Ion-Exchange/Dispersion Process in Porous Media. Paper 376, presented at AICHE 84th National Meeting, Atlanta, GA.

[27] Pope, G. A., & Nelson, R. C. (1978, October 1). A Chemical Flooding Compositional Simulator. Society of Petroleum Engineers. doi:10.2118/6725-PA.

[28] Hirasaki, G. J., van Domselaar, H. R., & Nelson, R. C. (1983, June 1). Evaluation of the Salinity Gradient Concept in Surfactant Flooding. Society of Petroleum Engineers. doi:10.2118/8825-PA.

[29] Flaaten, A. K., Nguyen, Q. P., Zhang, J., Mohammadi, H., & Pope, G. A. (2010, March 1). Alkaline/Surfactant/Polymer Chemical Flooding Without the Need for Soft Water. Society of Petroleum Engineers. doi:10.2118/116754-PA.

[30] Dwarakanath, V., Chaturvedi, T., Jackson, A., Malik, T., Siregar, A. A., & Zhao, P. (2008, January 1). Using Co-solvents to Provide Gradients and Improve Oil Recovery During Chemical Flooding in a Light Oil Reservoir. Society of Petroleum Engineers. doi:10.2118/113965-MS.

[31] Flaaten, A., Nguyen, Q. P., Pope, G. A., & Zhang, J. (2008, January 1). A Systematic Laboratory Approach to Low-Cost, High-Performance Chemical Flooding. Society of Petroleum Engineers. doi:10.2118/113469-MS.

[32] Zhang, J., Nguyen, Q. P., Flaaten, A., & Pope, G. A. (2008, January 1). Mechanisms of Enhanced Natural Imbibition with Novel Chemicals. Society of Petroleum Engineers. doi:10.2118/113453-MS.

[33] Kon, W., Pitts, M. J., & Surkalo, H. (2002, January 1). Mature Waterfloods Renew Oil Production by Alkaline-Surfactant-Polymer Flooding. Society of Petroleum Engineers. doi:10.2118/78711-MS.

[34] Sheng, J. J. (2013, April 19). A Comprehensive Review of Alkaline-Surfactant-Polymer (ASP) Flooding. Society of Petroleum Engineers. doi:10.2118/165358-MS.

[35] Jackson, A.C. (2006, December). Experimental Study of the Benefits of Sodium Carbonate on Surfactants for Enhanced Oil Recovery. MS thesis, The University of Texas at Austin, Austin, Texas, USA.

[36] Mohammadi, H., Delshad, M., & Pope, G. A. (2009, August 1). Mechanistic Modeling of Alkaline/Surfactant/Polymer Floods. Society of Petroleum Engineers. doi:10.2118/110212-PA.

[37] Nelson, R. C., Lawson, J. B., Thigpen, D. R., & Stegemeier, G. L. (1984, January 1). Cosurfactant-Enhanced Alkaline Flooding. Society of Petroleum Engineers. doi:10.2118/12672-MS.

[38] Martin, F. D., Oxley, J. C., & Lim, H. (1985, January 1). Enhanced Recovery of a "J" Sand Crude Oil With a Combination of Surfactant and Alkaline Chemicals. Society of Petroleum Engineers. doi:10.2118/14293-MS.

[39] Skrettingland, K., Holt, T., Tweheyo, M. T., & Skjevrak, I. (2011, April 1). Snorre Low-Salinity-Water Injection--

Coreflooding Experiments and Single-Well Field Pilot. Society of Petroleum Engineers. doi:10.2118/129877-PA.

[40] Mohammadi, H., & Jerauld, G. (2012, January 1). Mechanistic Modeling of the Benefit of Combining Polymer with Low Salinity Water for Enhanced Oil Recovery. Society of Petroleum Engineers. doi:10.2118/153161-MS.

[41] Ayirala, S., & Yousef, A. (2015, February 1). A State-of-the-Art Review To Develop Injection-Water-Chemistry Requirement Guidelines for IOR/EOR Projects. Society of Petroleum Engineers. doi:10.2118/169048-PA.

[42] Delshad, M., Han, C., Koyassan Veedu, F., & Pope, G. A. (2011, January 1). A Simplified Model for Simulations of Alkaline-Surfactant-Polymer Floods. Society of Petroleum Engineers. doi:10.2118/142105-MS.

[43] Goudarzi, A., Delshad, M., & Sepehrnoori, K. (2013, February 18). A Critical Assessment of Several Reservoir Simulators for Modeling Chemical Enhanced Oil Recovery Processes. Society of Petroleum Engineers. doi:10.2118/163578-MS.

[44] Kazemi Nia Korrani, A., Sepehrnoori, K., & Delshad, M. (2015, April 1). A Mechanistic Integrated Geochemical and Chemical-Flooding Tool for Alkaline/Surfactant/Polymer Floods. Society of Petroleum Engineers. doi:10.2118/169094-PA.

[45] Faber, M. J., Ameri, A., Farajzadeh, R., Bruining, H., Boersma, D. M., & Van Batenburg, D. W. (2013, July 2). Effect of Continuous, Trapped, and Flowing Gas on Performance of Alkaline Surfactant Polymer (ASP) Flooding. Society of Petroleum Engineers. doi:10.2118/165238-MS.

[46] Bhuyan, D. (1989). Development of an Alkaline/Surfactant/Polymer Compositional Reservoir Simulator. phD Dissertation, The University of Texas at Austin.

[47] Parkhurst, D. L., and Appelo, C. A. J. (2013). Description of Input and Examples for PHREEQC Version 3--a Computer Program for Speciation, Batch-reaction, One-dimensional Transport, and Inverse Geochemical Calculations.

[48] Khaledialidusti, R., Kleppe, J., & Skrettingland, K. (2015a, June 1). Numerical Interpretation of Single Well Chemical Tracer (SWCT) Tests to Determine Residual Oil Saturation in Snorre Reservoir. Society of Petroleum Engineers. doi:10.2118/174378-MS.

[49] Khaledialidusti, R., Kleppe, J., & Enayatpour, S. (2015b, September 14). Mechanistic Modeling of Alkaline/Surfactant/Polymer Floods Based on the Geochemical Reactions for Snorre Reservoir. Society of Petroleum Engineers. doi:10.2118/175655-MS.

[50] Bhuyan, D., Lake, L. W., & Pope, G. A. (1990, May 1). Mathematical Modeling of High-pH Chemical Flooding. Society of Petroleum Engineers. doi:10.2118/17398-PA.

[51] Korrani, A. K. N., Sepehrnoori, K., & Delshad, M. (2016, April 11). Significance of Geochemistry in Alkaline/Surfactant/Polymer (ASP) Flooding. Society of Petroleum Engineers. doi:10.2118/179563-MS.

[52] Hand. D.B. (1939). Dineric Distribution of a Consolute Liquid between Two immiscible Liquids. J. of Physics and Chemistry, Volume 34, pp. 1961-2000.

[53] Jin, M. (1995). A Study of Nonaqueous Phase Liquid Characterization and Surfactant Remediation. PhD dissertation, The University of Texas at Austin, Austin, Texas.

[54] Delshad, M., Delshad, M., Bhuyan, D., Pope, G. A., & Lake, L. W. (1986, January 1). Effect of Capillary Number on the Residual Saturation of a Three-Phase Micellar Solution. Society of Petroleum Engineers. doi:10.2118/14911-MS.

[55] Mohammadi, H. (2008, December). Mechanistic Modeling, Design, and Optimization of Alkaline/Surfactant/Polymer Flooding. PhD dissertation, The University of Texas at Austin, Austin, Texas.

[56] Novosad, Z., & Novosad, J. (1984, February 1). Determination of Alkalinity Losses Resulting From Hydrogen Ion Exchange in Alkaline Flooding. Society of Petroleum Engineers. doi:10.2118/10605-PA.

[57] Dezabala, E., Parekh, B., Solis, H. A., Choudhary, M. K., Armentrout, L. J., & Carlisle, C. T. (2011, January 1). Application of Single Well Chemical Tracer Tests to Determine Remaining Oil Saturation in Deepwater Turbidite Reservoirs. Society of Petroleum Engineers. doi:10.2118/147099-MS.

[58] Jerauld, G., Mohammadi, H., & Webb, K. J. (2010, January 1). Interpreting Single Well Chemical Tracer Tests. Society of Petroleum Engineers. doi:10.2118/129724-MS.

[59] Deans, H. A., & Carlisle, C. T. (1986, January 1). Single-Well Tracer Test in Complex Pore Systems. Society of Petroleum Engineers. doi:10.2118/14886-MS.

[60] De Zwart, A. H., van Batenburg, D. W., Stoll, M., Boerrigter, P. M., & Harthy, S. (2011, January 1). Numerical Interpretation of Single Well Chemical Tracer Tests for ASP injection. Society of Petroleum Engineers. doi:10.2118/141557-MS.

[61] Deans, H.A. (1971, November 30). Method of Determining Fluid Saturations in Reservoirs. U.S. Patent # 3623842.

[62] Tomich, J. F., Dalton, R. L., Deans, H. A., & Shallenberger, L. K. (1973, February 1). Single-Well Tracer Method To Measure Residual Oil Saturation. Society of Petroleum Engineers. doi:10.2118/3792-PA.

[63] Khaledialidusti, R., & Kleppe, J. (2016). A New Automated Algorithm for Designing the Optimal Single-Well-Chemical-Tracer SWCT Tests At Various Reservoir Conditions. Society of Petroleum Engineers. doi:10.2118/181612-MS.

[64] Khaledialidusti, R., Kleppe, J. & Enayatpour, S. (2016). Evaluation of surfactant flooding using interwell tracer analysis. J Petrol Explor Prod Technol. pp 1-20. doi:10.1007/s13202-016-0288-9.